



# A DFT perspective of potassium promotion of $\chi$ -Fe<sub>5</sub>C<sub>2</sub>(1 0 0)



Melissa A. Petersen<sup>a,b,\*</sup>, Muhammad J. Cariem<sup>b</sup>, Michael Claeys<sup>b</sup>, Eric van Steen<sup>b</sup>

<sup>a</sup> Sasol Technology (Pty) Ltd., R&D Division, 1 Klasie Havenga Road, Sasolburg 1947, South Africa

<sup>b</sup> Centre for Catalysis Research, Department of Chemical Engineering, University of Cape Town, Private Bag X3, Rondebosch 7701, South Africa

## ARTICLE INFO

### Article history:

Received 17 December 2014

Received in revised form 5 February 2015

Accepted 6 February 2015

Available online 19 February 2015

### Keywords:

DFT

Iron carbide

Promoter

Fischer–Tropsch synthesis

Adsorption

## ABSTRACT

Potassium is a well-known promoter for, amongst others, iron-based Fischer–Tropsch catalysts. Its effect is typically viewed in terms of the interaction of coadsorbed CO and zero-valent potassium, increasing the strength of CO adsorption with simultaneous weakening of the C–O bond. However, it is known that potassium also stabilises the adsorption of oxygen, which needs to be taken into consideration to evaluate the effect of potassium in a working Fischer–Tropsch catalyst. The presence of potassium results in a strong increase in the strength of adsorption of atomic oxygen on  $\chi$ -Fe<sub>5</sub>C<sub>2</sub>(1 0 0). The presence of atomic oxygen does not destabilise adsorbed CO at the coverage considered, and the strength of CO adsorption is significantly increased by the presence of coadsorbed K with or without coadsorbed atomic oxygen. The stabilisation of atomic oxygen due to the presence of coadsorbed potassium makes the removal of this species in the form of water under typical Fischer–Tropsch conditions difficult. Alternative pathways for the removal of atomic oxygen from the carbide surface are discussed.

© 2015 Elsevier B.V. All rights reserved.

## 1. Introduction

Alkali metals are well-known promoters for reactions taking place on metal surfaces, e.g. the ammonia synthesis, but also the Fischer–Tropsch synthesis. Alkali promotion of iron-based Fischer–Tropsch catalysts [1–3] results in enhanced catalytic activity together with enhanced carbon deposition, reduced methane selectivity, increased rate of CO<sub>2</sub> formation, increased chain growth and improved observed olefin selectivity. Potassium is usually used as the alkali of choice due to its cost-effectiveness [1,2]. The functioning of alkali as a promoter has been ascribed to electrostatic [4,5] and direct alkali–adsorbate interaction [6] resulting in an enhanced strength of adsorption of CO on metal surfaces due to the presence of potassium as e.g. shown theoretically for CO on Fe(1 0 0) [5,7] and more recently on Fe<sub>5</sub>C<sub>2</sub>(0 1 0) [8]. The short-range interaction between potassium and CO as the adsorbate was experimentally deduced using photon emission spectroscopy on Cu(1 1 1) and Ru(0 0 1) [9]. The enhanced strength of adsorption of CO and its enhanced rate of dissociation due to the presence of potassium have been experimentally confirmed using single crystal studies on Fe(1 1 0) [10], Fe(1 0 0) [11,12] and Fe(1 1 1) [13], and using polycrystalline iron [14], although the latter data must be

interpreted with some caution since the presence of potassium may stabilise higher Miller index planes [15], which may also contribute to an observed enhancement of the strength of CO adsorption.

Potassium does not only affect the physico-chemical properties of adsorbed CO, but also of other adsorbates [5,7,16]. It has been reported that potassium enhances the strength of adsorption of O adatoms [6,7,16], although oxygen is primarily bonded to the metal and not to potassium [16].

Coadsorption of oxygen and CO on Fe(1 0 0) has been observed to reduce the strength of CO adsorption [11], as has also been found on Ru(0 0 1) [17], Pt(1 1 1) [18], Pd(1 1 1) [19], and Rh(1 1 1) [20]. The diminished heat of adsorption of CO in the presence of O has been linked to a reduced electron donation from the metal substrate into the 2π\*-orbital of CO [11,17], which may lead to a change in its preferred adsorption site [19]. The frequency for C–O stretching increases upon coadsorption of oxygen [17,20], which can be taken as an indication for the observed inhibition of CO dissociation [11].

The contrasting effect of potassium and oxygen on the adsorption of CO on a surface raises the question as to the combined effect of both adsorbates on the adsorption of CO. Furthermore, a strong adsorption of oxygen on the carbide surface may have mechanistic implications on the working of the iron-based Fischer–Tropsch catalyst. A strengthening of the adsorption of atomic oxygen on the catalytic active surface may enhance the oxidation of the catalytically active carbide phase [1,21,22]. Here, we report on a density functional theory (DFT) study of the combined effect of oxygen, carbon monoxide and potassium on an iron carbide surface and draw

\* Corresponding author at: Sasol Technology (Pty) Ltd., R&D Division, 1 Klasie Havenga Road, Sasolburg 1947, South Africa. Tel.: +27 216505344.  
E-mail address: [melissa.petersen@sasol.com](mailto:melissa.petersen@sasol.com) (M.A. Petersen).

in particular attention to the consequences for iron-based catalysts under realistic Fischer–Tropsch conditions.

## 2. Computational method

The adsorption and coadsorption of CO, O and K were investigated on the  $\chi$ -Fe<sub>5</sub>C<sub>2</sub>(100)<sub>0,0</sub> surface (i.e. cut through the origin, following the notation of Steynberg et al. [23]), which is one of the many surface orientations thought to be present during Fischer–Tropsch synthesis [24]. The iron-rich  $\chi$ -Fe<sub>5</sub>C<sub>2</sub>(100)<sub>0,0</sub> surface is a corrugated surface exposing two unique surface iron atoms found on the ‘ridge’ and in the ‘valley’ of the surface, two distinct threefold hollow sites, one fourfold hollow site with a central sub-surface carbon atom, and five bridge (br) sites, as shown in Fig. 1a. A  $p(2 \times 1)$  surface unit cell was chosen, since this is expected to reduce the lateral interactions between adsorbates in adjacent unit cells [7], but more importantly the optimum level of potassium doping is believed [25] to be in the range of 1–2 K/nm<sup>2</sup>. This is equivalent to 1 potassium atom in a  $p(2 \times 1)$  surface unit cell of  $\chi$ -Fe<sub>5</sub>C<sub>2</sub>(100)<sub>0,0</sub>.

Spin-polarised DFT calculations were performed as implemented in VASP [26,27]. The exchange–correlation energy was calculated using the RPBE [28] functional together with the projector augmented wave (PAW) method to describe the electron–ion interactions [27,29]. In particular for potassium, the 3s and 3p semi-core states were explicitly treated as valence states in the calculations. The sampling of the Brillouin zone was performed using the Monkhorst–Pack scheme [30] with a  $k$ -point mesh of  $3 \times 5 \times 1$  for the  $p(2 \times 1)$  unit cell. Methfessel–Paxton smearing [31] to the first order was employed with a smearing width of 0.1 eV. A cut-off energy of 400 eV for expansion of the plane wave basis set was used. These parameters have been demonstrated to provide adequate energy convergence in previous studies of the iron carbide system [32].

The  $\chi$ -Fe<sub>5</sub>C<sub>2</sub>(100)<sub>0,0</sub> surface was represented by a slab consisting of 10 Fe-layers and 4 C-layers (see Fig. 1b). For the  $p(2 \times 1)$  unit cell, the slab is therefore equivalent to two conventional bulk units of  $\chi$ -Fe<sub>5</sub>C<sub>2</sub>. For monoclinic Hägg iron carbide, lattice parameters of  $a = 11.627$  Å,  $b = 4.551$  Å,  $c = 5.034$  Å and  $\beta = 97.81^\circ$  were calculated for the conventional bulk unit cell, deviating by less than 1% from the experimental parameters of  $a = 11.588$  Å,  $b = 4.579$  Å,  $c = 5.059$  Å and  $\beta = 97.746^\circ$  reported by Retief [33]. We note, however, that more recent experimental characterisation of the crystal structure points to a triclinic structure [34], and limitations in the description of the bulk unit cell by DFT has been addressed previously [23,35].

The adsorbates, CO, O and K, were positioned on one side of the slab, and the atomic coordinates of the adsorbates, together

with the top 4 Fe-layers and the top C-layer of the  $\chi$ -Fe<sub>5</sub>C<sub>2</sub>(100)<sub>0,0</sub> slab were optimised by minimising the forces on the unconstrained atoms to less than 0.03 eV/Å. All reported energies include a zero point energy (ZPE) correction calculated from the vibrational frequencies as determined from the mass-weighted Hessian matrix. The Hessian matrix was obtained by perturbing the adsorbate atoms by 0.02 Å in the direction of each of the Cartesian coordinates, while keeping the substrate atoms fixed at their optimised positions. A dipole correction perpendicular to the surface was applied, as implemented in the VASP code. A vacuum layer distance of 12 Å between neighbouring slabs was utilised for the systems without potassium. Systems involving potassium contained a vacuum layer of 20 Å between the slabs representing a compromise between computational time and the convergence of the calculated adsorption energies: the calculated adsorption energy of atomic K on Fe<sub>5</sub>C<sub>2</sub>(100)<sub>0,0</sub> in a  $p(2 \times 1)$  unit cell is –1.62 eV including a dipole correction of 0.08 eV with a vacuum spacing of 20 Å, and is –1.65 eV including a dipole correction of 0.04 eV for a vacuum spacing of 30 Å. Atom-resolved charges were calculated using the method due to Bader [36], with the algorithms developed by Henkelman et al. [37] and including the core charge density in the partitioning. Calculated properties of gas phase CO, H<sub>2</sub> and H<sub>2</sub>O are summarised in Table S1 of the Supplementary information.

## 3. Results and discussion

### 3.1. CO adsorption on $\chi$ -Fe<sub>5</sub>C<sub>2</sub>(100)<sub>0,0</sub>

The optimum configuration of CO adsorbed in a  $p(2 \times 1)$  cell of the  $\chi$ -Fe<sub>5</sub>C<sub>2</sub>(100)<sub>0,0</sub> surface was explored by considering a variety of starting geometries, viz. the atop position on iron on the ridge, the atop position on iron in the valley, the two inequivalent threefold hollow sites, the fourfold hollow site and the five bridge sites (Fig. 1). Only three stable positions were found for CO adsorption, viz. an atop position on the iron on the ridge (Fig. 2a), a bridge site (br2) between iron atoms on the ridge (Fig. 2b) and a bridge site (br5) between iron on the ridge and iron in the valley (Fig. 2c). Adsorption energies were calculated for each stable adsorption geometry according to the equation  $E_{\text{ads,CO}} = E_{\text{CO+slab}} - E_{\text{slab}} - E_{\text{CO}}$  where  $E_{\text{CO+slab}}$  is the energy (including the ZPE correction) of the Fe<sub>5</sub>C<sub>2</sub>(100)<sub>0,0</sub> slab with CO adsorbed on it,  $E_{\text{slab}}$  the energy of the clean Fe<sub>5</sub>C<sub>2</sub>(100)<sub>0,0</sub> slab and  $E_{\text{CO}}$  the energy of free CO with ZPE correction added.

Carbon monoxide adsorbs preferentially in the atop configuration on the ridge iron atoms with an adsorption energy of –1.57 eV. The C–O axis is tilted by 8° with respect to the surface normal of

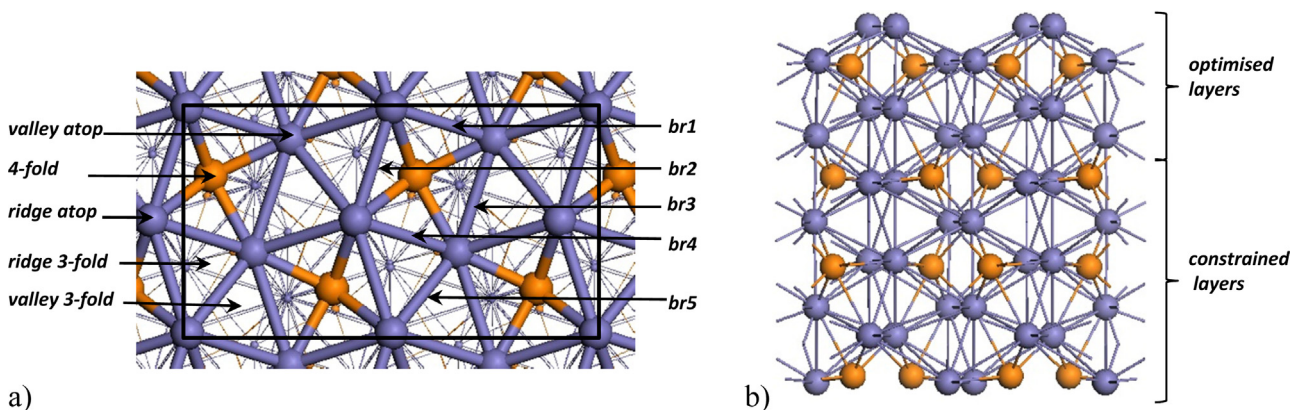


**Fig. 1.** (a) Top and (b) side views of the slab used to represent the  $\chi$ -Fe<sub>5</sub>C<sub>2</sub>(100)<sub>0,0</sub> surface. Unique adsorption sites are indicated in (a) together with the  $p(2 \times 1)$  surface unit cell. Layers of the slab that are constrained and optimised in calculations of the adsorbate geometries are indicated in (b). Iron atoms are purple and carbon atoms are orange.

Download English Version:

<https://daneshyari.com/en/article/39352>

Download Persian Version:

<https://daneshyari.com/article/39352>

[Daneshyari.com](https://daneshyari.com)